



# Resilience of transfluthrin to oxidative attack by duplicated CYP6P9 variants known to confer pyrethroid resistance in the major malaria mosquito *Anopheles funestus*

Melanie Nolden<sup>a,b</sup>, Robert Velten<sup>a</sup>, Mark J.I. Paine<sup>b</sup>, Ralf Nauen<sup>a,\*</sup>

<sup>a</sup> Bayer AG, Crop Science Division, Alfred Nobel Str. 50, D-40789 Monheim am Rhein, Germany

<sup>b</sup> Department of Vector Biology, Liverpool School of Tropical Medicine, Pembroke Place, Liverpool L3 5QA, United Kingdom

## ARTICLE INFO

### Keywords:

Cytochrome P450

Transfluthrin

CYP6P9a

CYP6P9b

Pyrethroids

*Anopheles*

## ABSTRACT

Resistance to common pyrethroids, such as deltamethrin and permethrin is widespread in the malaria mosquito *Anopheles funestus* and mainly conferred by upregulated cytochrome P450 monooxygenases (P450s). In the pyrethroid resistant laboratory strain *An. funestus* FUM0Z-R the duplicated genes *CYP6P9a* and *CYP6P9b* are highly upregulated and have been shown to metabolize various pyrethroids, including deltamethrin and permethrin. Here, we recombinantly expressed CYP6P9a and CYP6P9b from *An. funestus* using a baculovirus expression system and evaluated the interaction of the multifluorinated benzyl pyrethroid transfluthrin with these enzymes by different approaches. First, by Michaelis-Menten kinetics in a fluorescent probe assay with the model substrate 7-benzyloxymethoxy-4-trifluoromethylcoumarin (BOMFC), we showed the inhibition of BOMFC metabolism by increasing concentrations of transfluthrin. Second, we tested the metabolic capacity of recombinantly expressed CYP6P9 variants to degrade transfluthrin utilizing UPLC-MS/MS analysis and detected low depletion rates, explaining the virtual lack of resistance of strain FUM0Z-R to transfluthrin observed in previous studies. However, as both approaches suggested an interaction of CYP6P9 variants with transfluthrin, we analyzed the oxidative metabolic fate and failed to detect hydroxylated transfluthrin, but low amounts of an M-2 transfluthrin metabolite. Based on the detected metabolite we hypothesize oxidative attack of the gem-dimethyl substituted cyclopropyl moiety, resulting in the formation of an allyl cation upon ring opening. In conclusion, these findings support the resilience of transfluthrin to P450-mediated pyrethroid resistance, and thus, reinforces its employment as an important resistance-breaking pyrethroid in resistance management strategies to control the major malaria vector *An. funestus*.

## 1. Introduction

Malaria remains the most important vector-borne disease, especially in sub-Saharan Africa (SSA), transmitted by Anopheline mosquitoes of two species complexes, *Anopheles gambiae* s.l. and *Anopheles funestus* s.l. (Diptera: Culicidae). Out of an estimated 627,000 malaria deaths in 2020, >95% were reported from the African continent (WHO, 2021). *An. funestus* is one of the major malaria vectors in SSA (Coetzee and Koekemoer, 2013; Sinka et al., 2010), and its control mainly relies on the application of insecticides, particularly as indoor residual spray (IRS) and long-lasting insecticidal nets (LLINs) (Sinka et al., 2016). Although insecticide driven interventions, particularly pyrethroid-treated LLINs, largely contributed to a massive decrease of reported malaria cases

between 2000 and 2015 (Bhatt et al., 2015), an increased evolution of insecticide resistance has been observed (Hemingway et al., 2016; Ranson and Lissenden, 2016).

The insecticide portfolio to support vector control interventions is rather limited in terms of modes of action and chemical classes, so new high efficacy insecticides are urgently needed (Hoppé et al., 2016; Williams et al., 2019). Pyrethroids play a major role in Anopheline mosquito control, but high selection pressure resulted in increasing resistance levels jeopardizing the success of malaria control programs (Hemingway, 2018). Pyrethroids are fast acting insecticides targeting the insect neuronal voltage-gated sodium channels (VGSC) leading to rapid knock-down of the treated pests upon contact (Soderlund and Bloomquist, 1989). They are broadly divided into type I (e.g.

\* Corresponding author.

E-mail address: [ralf.nauen@bayer.com](mailto:ralf.nauen@bayer.com) (R. Nauen).

<https://doi.org/10.1016/j.pestbp.2023.105356>

Received 20 December 2022; Received in revised form 20 January 2023; Accepted 25 January 2023

Available online 2 February 2023

0048-3575/© 2023 The Author(s). Published by Elsevier Inc. This is an open access article under the CC BY-NC-ND license (<http://creativecommons.org/licenses/by-nc-nd/4.0/>).

permethrin) and type II pyrethroids (e.g. deltamethrin), depending on the absence and presence of an  $\alpha$ -cyano group, respectively (Soderlund, 2020). Transfluthrin (2,3,5,6-tetrafluorobenzyl(1R,3S)-3-(2,2-dichlorovinyl)-2,2-dimethylcyclopropane-carboxylate; syn. benfluthrin) is a volatile, enantiomerically pure type I pyrethroid, with a multi-fluorinated benzyl moiety instead of the more common 3-phenoxybenzyl moiety (Khambay, 2002). It exhibits good contact activity against adult mosquitoes (Horstmann and Sonneck, 2016), and has been shown to lack cross-resistance to 3-phenoxybenzyl substituted pyrethroids such as deltamethrin and cypermethrin in *An. funestus* strain FUMOZ-R (Nolden et al., 2021).

Pyrethroid insecticide resistance in pest insects, including vectors of human diseases, is predominantly conferred by target-site mutations in the VGSC, i.e., amino acid substitutions affecting pyrethroid binding (Rinkevich et al., 2013; Scott, 2019), and increased detoxification driven by the constitutive overexpression and/or duplication of genes of metabolic enzymes, particularly cytochrome P450-monooxygenases (P450s) (Nauen et al., 2022; Vontas et al., 2020). In *An. funestus* resistance against different pyrethroid chemotypes has been shown to be conferred by upregulated P450s, but not target-site resistance (Irving and Wondji, 2017; Riveron et al., 2014; Wondji et al., 2009, 2022). Several *An. funestus* P450s were functionally expressed and shown to metabolize various pyrethroids, such as permethrin (type I) and deltamethrin (type II) (Ibrahim et al., 2018; Riveron et al., 2013, 2014, 2017; Wamba et al., 2021). Among those P450s recombinantly expressed, especially CYP6P9a and CYP6P9b are playing a key role in pyrethroid resistance in *An. funestus*, including the resistant laboratory reference strain FUMOZ-R originating from Mozambique (Nolden et al., 2022a; Williams et al., 2019; Wondji et al., 2022). Previous work revealed that common phenoxybenzyl-pyrethroids, such as deltamethrin are primarily hydroxylated at the 4' para position of the phenoxybenzyl-ring, as for example shown for CYP6M2 of *An. gambiae* (Stevenson et al., 2011). The same authors also demonstrated that 4'OH deltamethrin is further metabolized by the same enzyme resulting in the formation of cyano(3-hydroxyphenyl) methyl deltamethrate. Very recently, sequential metabolism of both deltamethrin and permethrin via hydroxylation followed by ether cleavage has been demonstrated in studies employing recombinantly expressed CYP6P9a and CYP6P9b of *An. funestus* (Nolden et al., 2022b).

We recently demonstrated that *An. funestus* strain FUMOZ-R lacks phenotypic cross-resistance to transfluthrin when compared to a susceptible reference strain, FANG. However, increased adult toxicity (synergism) has been observed in glazed tile bioassays in combination with P450 inhibitors such as piperonyl butoxide, principally suggesting oxidative metabolism of transfluthrin (Nolden et al., 2021). The objective of this study was to investigate the metabolic capacity of recombinantly expressed CYP6P9a and CYP6P9b to degrade transfluthrin by various approaches, including fluorescent probe competition assays and UPLC-MS/MS analysis to elucidate transfluthrin depletion rates and potential metabolites.

## 2. Material and methods

### 2.1. Chemicals

Transfluthrin (CAS: 118712-89-3),  $\beta$ -Nicotinamide adenine dinucleotide 2'-phosphate (NADPH) reduced tetrasodium salt hydrate (CAS: 2646-71-1 anhydrous, purity  $\geq 93\%$ ) and 7-hydroxy-4-trifluoromethylcoumarin (HFC; CAS: 575-03-1, 98) were purchased from Sigma Aldrich/Merck (Darmstadt, Germany). Transfluthrin derivatives TF-0, TF-1, TF-3, and TF-5 were of analytical grade and obtained internally from Bayer (Leverkusen, Germany). NADPH regeneration system (V9510) was purchased from Promega (Madison, USA). 7-benzoyloxymethoxy-4-trifluoromethylcoumarin (BOMFC; CAS: 277309-33-8; purity 95%) was synthesized by Enamine Ltd. (Riga, Latvia). All other chemicals and solvents were of analytical grade and purchased from Sigma/

Aldrich (Darmstadt, Germany) unless otherwise stated.

### 2.2. Heterologous expression of CYP6P9a and CYP6P9b

CYP6P9a (VectorBase ID: AFUN015792) and CYP6P9b (AFUN015889) were recombinantly co-expressed with NADPH cytochrome P450 reductase (CPR) from *An. gambiae* (GenBank: AY183375.1; Table S1) in High-5 insect cells as previously described (Nolden et al., 2022a). In brief: PFastBac1 vectors containing each gene of interest - codon optimized for expression in lepidopteran cell lines - were created employing the GeneArt server (ThermoFisher, Waltham, MA, USA). Plasmids were transformed using MaxEfficiencyDH10 (Invitrogen, Waltham, MA, USA) according to manufacturer instructions and isolated using large construct kit (Qiagen, Hilden, Germany) following standard protocols. The recombinant baculovirus DNA was constructed and transfected into *Trichoplusia ni* High-5 cells using the Bac-to-Bac baculovirus expression system as described elsewhere (Manjon et al., 2018). CYP6P9a and CYP6P9b were co-expressed with *An. gambiae* CPR with a multiplicity of infection (MOI) of 1 (P450): 0.5 (CPR). High-5 cells were diluted to  $1.5 \times 10^6$  cells/mL and incubated with 0.5% fetal bovine serum (FBS), 0.2 mM *delta*-aminolevulinic acid (*d*-ALA), 0.2 mM iron (III) citrate and the respective amount of virus for 52 h at 27 °C and 120 rpm. After harvesting, cells were resuspended in homogenization buffer (0.1 M K<sub>2</sub>HPO<sub>4</sub>, 1 mM DTT, 1 mM EDTA, 200 mM sucrose, pH 7.6). FastPrep device (MP Biomedicals, Irvine, CA, USA) was used for grinding the cells following a 10 min centrifugation step at 4 °C and 700 g. The resulting supernatant was centrifuged for one hour at 100,000 g and 4 °C. Afterwards the microsomal pellet was resuspended with a Dounce tissue grinder in buffer (0.1 M K<sub>2</sub>HPO<sub>4</sub>, 0.1 mM EDTA, 1 mM DTT, 5% glycerol, pH 7.6). The amount of protein was measured using Bradford reagent (Bradford, 1976).

### 2.3. Fluorescent probe assays using BOMFC

Inhibition assays were conducted with minor changes as described previously (Nolden et al., 2022a). In brief: recombinantly expressed CYP6P9a and CYP6P9b were diluted in buffer (0.1 M K<sub>2</sub>HPO<sub>4</sub>, 0.1 mM EDTA, 1 mM DTT, 5% glycerol pH 7.6), incl. 0.05% bovine serum albumin (BSA) and 0.01% zwittergent 3-10 to 0.16 mg/mL. BOMFC (stock solution 50 mM in DMSO) was diluted to eleven different concentrations ranging from 200  $\mu$ M to 0.0195  $\mu$ M (final assay concentration (fc)) in assay buffer (0.1 M potassium-phosphate buffer (pH 7.6), containing 0.01% zwittergent 3-10 and different pyrethroid concentrations with and without 1 mM NADPH. Twenty-five  $\mu$ L of enzyme solution, corresponding to 4  $\mu$ g total protein, were incubated with 25  $\mu$ L of substrate solution in black 384-well plates (Fluotrac, Greiner bio-one, Belgium) for one hour at  $20 \pm 1$  °C. Each reaction was replicated four times and the fluorescent product HFC was measured at 405 nm while excited at 510 nm. Substrate saturation kinetics (Michaelis-Menten plots) and enzyme inhibition were analyzed by non-linear regression using GraphPad Prism 9.0 (GraphPad Software, San Diego, Ca, USA). IC<sub>50</sub> values were calculated to express the inhibition of BOMFC O-debenzylation by different pyrethroids.

### 2.4. UPLC-MS/MS analysis

Analysis of transfluthrin metabolism by CYP6P9a and CYP6P9b was conducted as described previously (Nolden et al., 2022b) with minor modifications. Forty  $\mu$ L of recombinantly expressed CYP6P9a and CYP6P9b, diluted to 0.8 mg protein mL<sup>-1</sup> in buffer (0.1 M K<sub>2</sub>HPO<sub>4</sub>, 1 mM DTT, 0.1 mM EDTA, 5% Glycerol, pH 7.6, containing 0.05% BSA) were incubated with 10  $\mu$ L of 10  $\mu$ M (fc) transfluthrin (diluted in 0.1 M K<sub>2</sub>HPO<sub>4</sub>, 0.05% bovine serum albumin (BSA), pH 7.6) and 50  $\mu$ L assay buffer (0.1 M K<sub>2</sub>HPO<sub>4</sub>, pH 7.6) with and without NADPH regeneration system in 1 mL 96-deepwell plates (Protein-LoBind, Eppendorf). Microsomal fractions from High-5 cells infected with virus containing

PFastbac1 vector with no inserted DNA served as control. Each reaction was replicated four times and incubated for 90 min at 30 °C and 450 rpm (Thermomixer, Eppendorf). The reactions were stopped with 400  $\mu$ L ice-cold acetonitrile (100%), incubated at 4 °C overnight, and centrifuged for 30 min at 3000 g and 4 °C. The resulting supernatant was analyzed using an Agilent 1290 Infinity II UPLC system, equipped with a Waters Acquity BEH C18 column (2.1  $\times$  50 mm, 1.7  $\mu$ m). Chromatography was carried out using 2 mM ammonium-acetate in methanol and 2 mM ammonium-acetate in water including 1% acetic acid as the eluent in gradient mode. After positive electrospray ionization, ion transitions were recorded on a Sciex API6500 Qtrap. Transfluthrin was measured in positive ion mode (ion transition: transfluthrin 371 > 163). The linear range for transfluthrin quantification was 0.5–200 ng/mL.

## 2.5. Metabolite analysis

UPLC-TOF-MS was employed using an Acquity UPLC I-Class system coupled to a cyclic iMS mass spectrophotometer (Waters Corporation, MA, USA). A Zorbax Eclipse Plus C18 column (2.1  $\times$  100 mm, 1.8  $\mu$ m) (Agilent Technologies, CA, USA) was used with a column oven temperature of 60 °C. The mobile phase consisted of acetonitrile/0.25% formic acid (eluent A) and water/0.25% formic acid (eluent B) in gradient mode and a flow rate of 0.6 mL min<sup>-1</sup> with eluent B starting at 90% for 4.5 min, decreasing to 5% for 2.5 min and increasing to 90% again for 1 min. The mass spectrometer operated in positive ion mode with a full scan resolution of 60,000 fwhm (full width at half maximum). Measurements and metabolite search were conducted with MassLynx and Metabolynx software (Waters Corporation, MA, USA).

## 2.6. Cheminformatic analysis

Minimum energy conformer alignments and three-dimensional ball-and-stick models of transfluthrin and deltamethrin in standard normalized orientation were generated using the software package Maestro (Schroedinger Release 2020–1; Maestro Schroedinger LLC, New York, NY, USA). Isosurfaces of the Fukui functions for attack by an electrophile as calculated from DFT (density functional theory) densities were done as described elsewhere (Beck, 2005).

## 3. Results

### 3.1. Fluorescent probe competition assays

Transfluthrin and its defluorinated benzyl derivative TF-0 showed IC<sub>50</sub>-values for the inhibition of the O-debenzylation of BOMFC by recombinantly expressed CYP6P9a and CYP6P9b at similar micromolar concentrations (Table 1), therefore, principally suggesting interaction with the catalytic site of both P450s. Deltamethrin and the two other tested transfluthrin derivatives, TF-1 and TF-5 (Fig. 1), exhibited IC<sub>50</sub>-values of >100  $\mu$ M, suggesting a weaker interaction with both enzymes

**Table 1**

Interaction of pyrethroids with CYP6P9a and CYP6P9b. Inhibition of BOMFC O-debenzylation by recombinantly expressed CYP6P9a and CYP6P9b by transfluthrin, TF-5, TF-1 and TF-0 (for chemical structures refer to Fig. 1). Data are mean values  $\pm$  CI 95% (n = 4). Deltamethrin data was taken from Nolden et al., 2022b.

Compound	CYP6P9a		CYP6P9b	
	IC <sub>50</sub> ( $\mu$ M)	95% CI*	IC <sub>50</sub> ( $\mu$ M)	95% CI*
Transfluthrin	66.3	50.3–92.6	69.9	49.6–105
TF-0	44.7	38.2–52.8	70.2	52–103
TF-5	> 100 $\mu$ M		> 100 $\mu$ M	
TF-1	> 100 $\mu$ M		> 100 $\mu$ M	
Deltamethrin	> 100 $\mu$ M		> 100 $\mu$ M	

\* 95% confidence intervals.

(Table 1).

Steady-state kinetic analyses of the O-debenzylation of BOMFC by recombinantly expressed CYP6P9a and CYP6P9b in the absence and presence of different concentrations of transfluthrin are shown in Fig. 2. Further studies revealed a mixed type competitive/non-competitive inhibition (Table S2) based on kinetic characteristics of reversible P450 inhibition models (Fowler and Zhang, 2008). At the highest tested transfluthrin concentration of 100  $\mu$ M the K<sub>m</sub>-value for BOMFC significantly increased for both CYP6P9a and CYP6P9b, whereas the V<sub>max</sub> values significantly decreased compared to co-incubations with 1  $\mu$ M transfluthrin (Table S2).

### 3.2. Metabolism of transfluthrin by recombinantly expressed CYP6P9a and CYP6P9b

UPLC-MS/MS analysis revealed modest depletion of transfluthrin when incubated with recombinantly expressed CYP6P9 variants in the presence of NADPH in comparison to the control (empty virus, expressed in High-5 cells), and CYP6P9 variants in the absence of NADPH (Fig. 3A). We observed no difference in the depletion of transfluthrin between microsomal membrane preparations expressing CYP6P9a or CYP6P9b (Table S3), confirming the results obtained in fluorescent probe competition assays (Table 1). Thus, suggesting that both enzymes exhibit the same capacity to interact with transfluthrin. Interestingly, we detected a significant depletion of transfluthrin between control-virus and microsomal membranes containing CYP6P9 variants but incubated in the absence of NADPH, most likely indicating sequestration. Metabolite identification employing UPLC-TOF-MS revealed the presence of DCCA, 3-(2,2-dichlorovinyl)-2,2-dimethylcyclo-propane-carboxylic acid (M-162; Fig. S1), at very low levels in all samples, except those prepared from transfluthrin incubations without microsomal membranes, suggesting transfluthrin hydrolysis by microsomal preparations of High-5 cells irrespective of the expression of CYP6P9 variants and the presence or absence of NADPH. In addition, we identified a single M-2 metabolite (Fig. 3B) specifically when recombinantly expressed CYP6P9a and CYP6P9b were incubated with transfluthrin in the presence of NADPH, but not in the absence of the co-factor. We failed to detect an M + 16 signal - indicative for a stable hydroxy metabolite - in any of the samples. The formation of the M-2 metabolite by both CYP6P9a and CYP6P9b likely explains the observed significant difference in oxidative transfluthrin metabolism in the presence and absence of NADPH shown in Fig. 3A.

Based on these results, we suggest the hydroxylation of one of the methyl groups of the gem-dimethyl substituted cyclopropyl moiety, resulting in the formation of an intermediate allyl cation upon ring opening. Elimination of a proton results in the chemically stable M-2 metabolite proposed in Fig. 4. A cheminformatic analysis of local reactivity descriptors by calculating the isosurfaces of the Fukui function (Beck, 2005) for an electrophilic attack of transfluthrin revealed the maximum of the Fukui function at the gem-dimethyl cyclopropyl moiety (Fig. 5), providing *in-silico* support for the proposed oxidative metabolic fate of transfluthrin catalyzed by *An. funestus* CYP6P9a and CYP6P9b.

## 4. Discussion

Transfluthrin is a multifluorinated benzyl pyrethroid which has been recently shown to virtually lack cross-resistance to common phenox-ybenzyl pyrethroids such as deltamethrin and permethrin in *An. funestus* strain FUM0Z-R (Horstmann and Sonneck, 2016). When compared to the susceptible reference strain FANG, FUM0Z-R exhibited resistance ratios of >220-fold and 2.5-fold for deltamethrin and transfluthrin, respectively (Nolden et al., 2021). Previous studies demonstrated that the overexpression of duplicated P450s, CYP6P9a and CYP6P9b, confers high levels of pyrethroid resistance in *An. funestus* (Wondji et al., 2009, 2022), which has been confirmed for various pyrethroids by metabolism studies after functional expression of these enzymes (Nolden et al.,

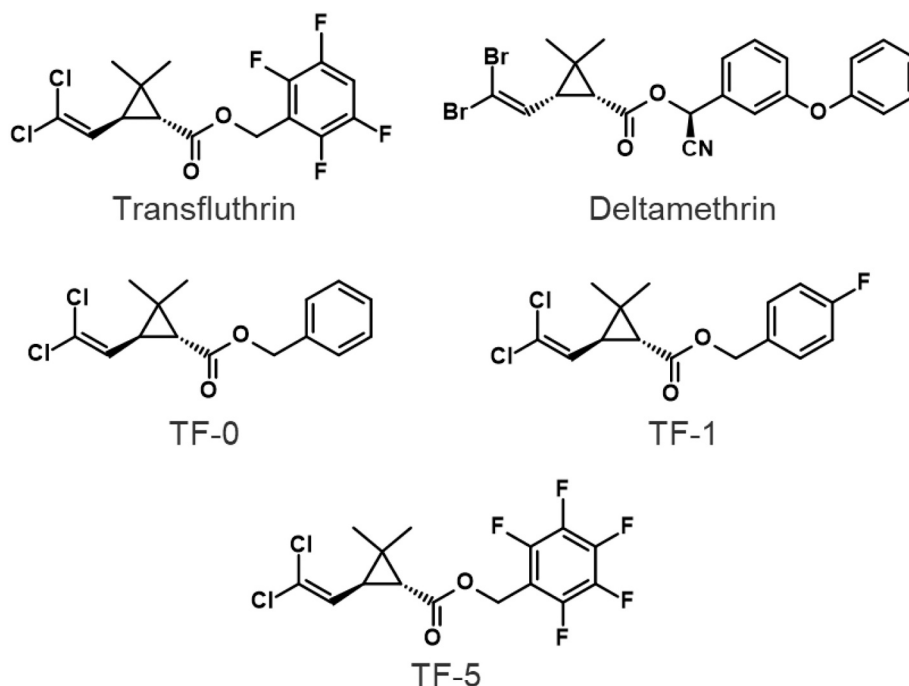


Fig. 1. Chemical structures of deltamethrin, transfluthrin and its derivatives used in this study.

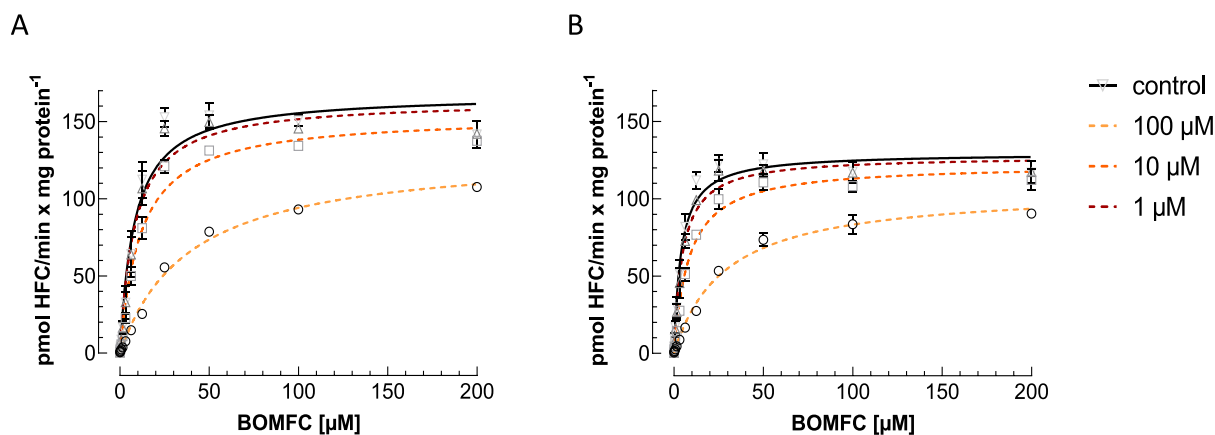


Fig. 2. Effect of transfluthrin on the *O*-debenzylation of 7-benzyloxymethoxy-4-(trifluoromethyl)-coumarin (BOMFC) by recombinantly expressed *An. funestus* CYP6P9 variants. Michaelis–Menten kinetics of (A) CYP6P9a- and (B) CYP6P9b-mediated BOMFC metabolism at increasing concentrations of transfluthrin. Data are mean values  $\pm$  SD (n = 4). Reaction velocity is defined as pmol 7-hydroxy-4-trifluoromethylcoumarin (HFC) / min x mg protein. Details on Michaelis-Menten kinetic based data analysis are given in the Supporting Information, table S2.

2022b; Riveron et al., 2013), whereas their metabolic capacity to interact with transfluthrin remains elusive.

Here we demonstrated by various approaches that recombinantly expressed CYP6P9a and CYP6P9b interact with transfluthrin and its non-fluorinated derivative TF-0. Transfluthrin (and TF-0) at mid-micromolar concentrations inhibited the *O*-debenzylation of the fluorescent probe substrate BOMFC by CYP6P9 variants. This provides a first line of evidence that transfluthrin binds to the active site of these enzymes and is possibly metabolized, as for example previously shown for hydroxylated phenoxybenzyl pyrethroids as products of the sequential metabolism of deltamethrin and permethrin, which themselves did not inhibit CYP6P9 variants (Nolden et al., 2022b). Interestingly, in another study, deltamethrin showed tight interaction with diethoxyfluorescein binding and its *O*-deethylation in fluorescent probe assays with *An. funestus* CYP6P9a and CYP6P9b (Ibrahim et al., 2015), whereas BOMFC (*O*-debenzylation) as a substrate failed to detect such an interaction with

deltamethrin in the present and previous studies (Nolden et al., 2022b), suggesting that fluorescent substrates behave differently depending on the reaction type. Other P450s such as *An. gambiae* CYP6Z2 have been demonstrated to tightly bind deltamethrin but lack the capacity to metabolize it (McLaughlin et al., 2008). Considering these results, it is difficult to predict the metabolization of a pyrethroid insecticide solely based on inhibition data obtained in fluorescent probe assays with recombinantly expressed P450s. In contrast, similar fluorescent probe assays with P450s from other insect species such as whiteflies (CYP6CM1) and honeybees (e.g., CYP9Q3) have been predictive for the metabolism of a range of insecticidal chemotypes such as neonicotinoids, butenolides and diamides (Haas et al., 2021, 2022; Hamada et al., 2019). Future work is warranted to better understand the predictive power of such biochemical assays using recombinantly expressed P450s.

Next, we investigated the capacity of CYP6P9a and CYP6P9b to

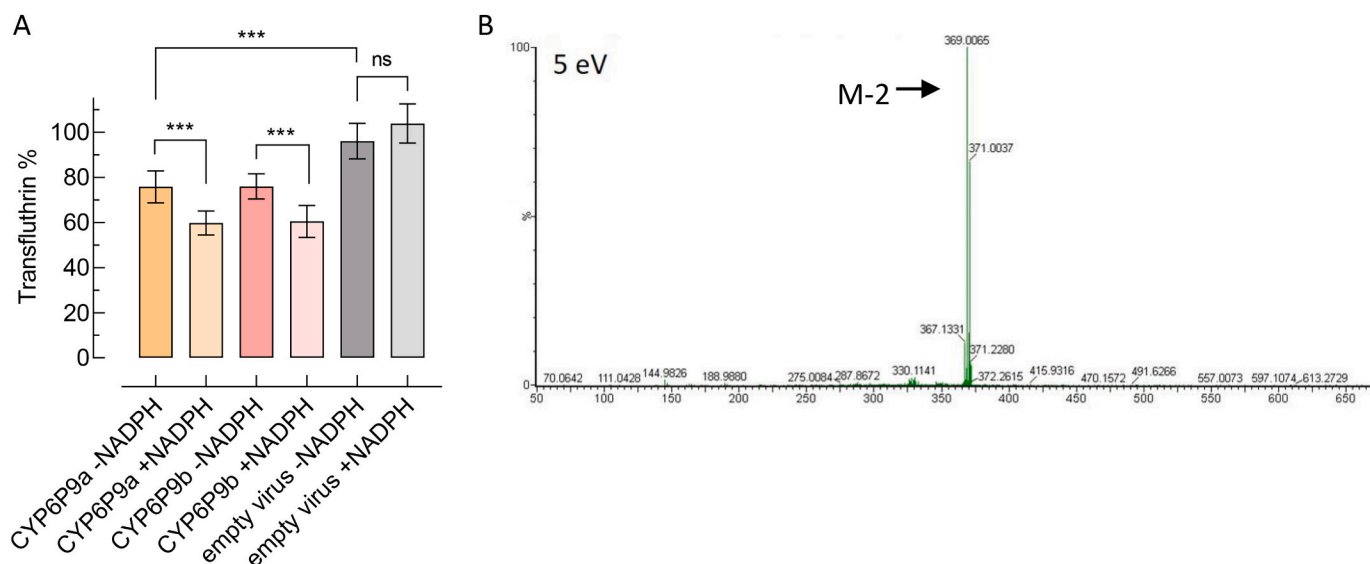


**Fig. 3.** Transfluthrin metabolism by recombinantly expressed *An. funestus* CYP6P9 variants in vitro. (A) Transfluthrin remaining after 90 min incubation at 30 °C with CYP6P9a and CYP6P9b, with and without NADPH. Empty virus served as control. Data are mean values  $\pm$  CI 95% ( $n = 6$ ). (B) ESI-TOF high resolution MS/MS spectrum of the M-2 metabolite detected after incubation of transfluthrin with recombinantly expressed CYP6P9 variants in the presence of NADPH.

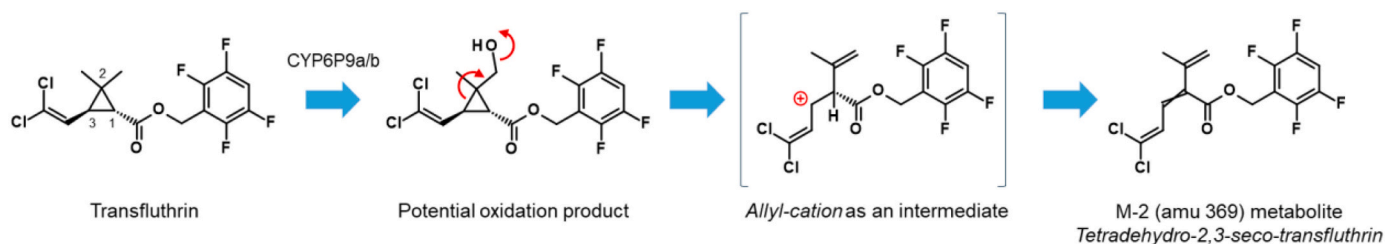


**Fig. 4.** Oxidative metabolism of transfluthrin. Proposed scheme for the oxidative metabolism of transfluthrin by *An. funestus* CYP6P9a and CYP6P9b based on a transfluthrin metabolite (M-2) detected by UPLC-MS/MS.

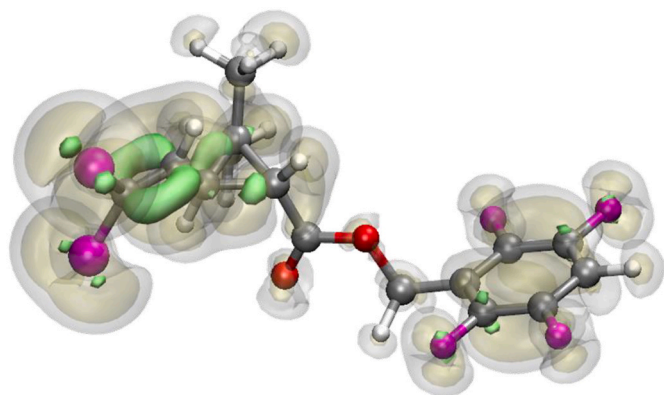


**Fig. 5.** Cheminformatic modelling approaches. Isosurfaces of the Fukui functions for attack by an electrophile (green, solid; isolevel 0.05 au) as calculated from DFT densities for transfluthrin according to Beck (2005). (For interpretation of the references to colour in this figure legend, the reader is referred to the web version of this article.)

metabolize transfluthrin by employing UPLC-MS/MS and UPLC-TOF-MS analysis and detected two different metabolites, transfluthrin M-162 and transfluthrin M-2. Transfluthrin M-162 has been detected in all samples at low levels, except those lacking High-5 cell microsomal membranes, indicating an inherent capacity of High-5 cell microsomes to metabolize transfluthrin. The M-162 metabolite is known to represent DCCA

(Yoshida, 2014), i.e., the acid moiety of transfluthrin resulting from its hydrolysis along with 2,3,5,6-tetrafluorobenzyl alcohol, representing the alcohol moiety of transfluthrin (Fig. S1). Interestingly, High-5 cells originate from cabbage looper, *Trichoplusia ni*, which has been previously shown to partially metabolize permethrin by microsomal hydrolysis, resulting in DCCA and 3-phenoxybenzylalcohol (Shono et al., 1979). DCCA is also a major metabolite in urinary excretions of rats administered transfluthrin (Yoshida, 2012). In a recent study with *Cunninghamella* spp., a fungi routinely used to model drug metabolism, it has been shown that the microsomal hydrolysis of transfluthrin is prevented by the addition of 1-aminobenzotriazole (Khan and Murphy, 2021), a well-described P450 inhibitor (de Montellano, 2018). Suggesting that most likely P450 activity in *Cunninghamella* spp. is mediating the hydrolysis of the ester bond of transfluthrin. However, whether the detected DCCA levels in our study reflect microsomal hydrolysis of transfluthrin by High-5 cell P450s remains to be tested in future studies.

One of the major routes of oxidative pyrethroid metabolism is 4hydroxylation of the phenoxybenzyl moiety (Khambay and Jewess, 2004). This route has been described for deltamethrin, permethrin, cypermethrin and other pyrethroids in mammalian and insect microsomal preparations (Anand et al., 2006; Scollon et al., 2009; Shono et al., 1979). Recombinantly expressed mosquito P450s such as *An. gambiae* CYP6M2 and *An. funestus* CYP6P9a/b have been shown to sequentially metabolize deltamethrin and permethrin by 4hydroxylation and phenoxybenzyl ether cleavage (Nolden et al., 2022b; Stevenson et al., 2011). In the present study we failed to detect a hydroxylated M + 16 transfluthrin metabolite, confirming the hypothesis that the *para*-position of the multifluorinated benzyl ring is protected from oxidative

attack by P450s (Horstmann and Sonneck, 2016). Our study further supports this claim by fluorescent probe competition assays and the lack of interaction of CYP6P9 variants with the transfluthrin derivatives TF-1 and TF-5, which are fluorinated at the benzyl *para*-position. Instead, we detected a transfluthrin M-2 metabolite at low, but significant amounts after incubation of CYP6P9a and CYP6P9b with transfluthrin. This M-2 metabolite has not been detected in the absence of the cofactor NADPH, strongly supporting its P450-catalyzed formation. We hypothesize that this stable metabolite, tetrahydro-2,3-*seco*-transfluthrin (Fig. 4), is formed by the oxidation of one of the methyl groups of the *gem*-dimethyl cyclopropyl moiety, followed by the elimination of a hydroxide ion, cationic cyclopropyl-methyl rearrangement and release of a proton (Suckling, 1988). Tetrahydro-2,3-*seco*-transfluthrin has been formally named by following IUPAC nomenclature and terminology (Favre and Powell, 2013). However, because we do not know the exact hydroxylation site at the transfluthrin *gem*-dimethyl moiety, we could not provide the exact stereochemistry of the formed double-bond. Hydroxylation of one of the *gem*-dimethyl groups has also been described for deltamethrin upon incubation with recombinantly expressed *An. gambiae* CYP6M2 (Stevenson et al., 2011), but not *An. funestus* CYP6P9 variants (Nolden et al., 2022b). Previous work with other pyrethroids and insect microsomal preparations demonstrated that the proposed *gem*-dimethyl site for P450-mediated oxidative attack provides a valid hypothesis as a potential route for transfluthrin degradation (Shono et al., 1979).

In conclusion, we propose that the limited capacity of CYP6P9 variants to catalyse this reaction, as demonstrated here by a very low depletion rate, likely explains the virtual lack of transfluthrin cross-resistance in *An. funestus* strain FUM0Z-R. Thus, qualifying transfluthrin as a valid option in resistance management strategies to control pyrethroid resistant populations of *An. funestus* under applied conditions.

## Declaration of Competing Interest

RN is employed by Bayer AG, a manufacturer of pesticides. MN is a PhD student affiliated with the LSTM and funded by the Innovative Vector Control Consortium (IVCC) and Bayer AG.

## Data availability

Data will be made available on request.

## Acknowledgements

We are grateful to Johannes Glaubitz, Heidrun Thalheim and Udo König for the analytical support regarding the identification of transfluthrin metabolites.

## Appendix A. Supplementary data

Supplementary data to this article can be found online at <https://doi.org/10.1016/j.pestbp.2023.105356>.

## References

- Anand, S.S., Bruckner, J.V., Haines, W.T., Muralidhara, S., Fisher, J.W., Padilla, S., 2006. Characterization of deltamethrin metabolism by rat plasma and liver microsomes. *Toxicol. Appl. Pharmacol.* 212 (2), 156–166. <https://doi.org/10.1016/j.taap.2005.07.021>.
- Beck, M.E., 2005. Do Fukui function maxima relate to sites of metabolism? A critical case study. *J. Chem. Inf. Model.* 45 (2), 273–282. <https://doi.org/10.1021/ci049687n>.
- Bhatt, S., Weiss, D.J., Cameron, E., Bisanzio, D., Mappin, B., Dalrymple, U., Battle, K.E., Moyes, C.L., Henry, A., Eckhoff, P.A., Wenger, E.A., Briet, O., Penny, M.A., Smith, T.A., Bennett, A., Yukich, J., Eisele, T.P., Griffin, J.T., Fergus, C.A., Gething, P.W., 2015. The effect of malaria control on *Plasmodium falciparum* in Africa between 2000 and 2015. *Nature* 526, 207–211.
- Bradford, M.M., 1976. A rapid and sensitive method for the quantitation of microgram quantities of protein utilizing the principle of protein-dye binding. *Anal. Biochem.* 72 (1) [https://doi.org/10.1016/0003-2697\(76\)90527-3](https://doi.org/10.1016/0003-2697(76)90527-3). Art. 1.
- Coetzee, M., Koekemoer, L.L., 2013. Molecular systematics and insecticide resistance in the major African malaria vector *Anopheles funestus*. *Annu. Rev. Entomol.* 58 (1) <https://doi.org/10.1146/annurev-ento-120811-153628>. Art. 1.
- de Montellano, P.R.O., 2018. 1-Aminobenzotriazole: a mechanism-based cytochrome P450 inhibitor and probe of cytochrome P450 biology. *Med. Chem.* 8 (3), 038. <https://doi.org/10.4172/2161-0444.1000495>.
- Favre, H.A., Powell, W.H., 2013. Nomenclature of organic. *Chemistry*. <https://doi.org/10.1039/9781849733069>.
- Fowler, S., Zhang, H., 2008. In vitro evaluation of reversible and irreversible cytochrome P450 inhibition: current status on methodologies and their utility for predicting drug-drug interactions. *AAPS J.* 10 (2), Art. 2. <https://doi.org/10.1208/s12248-008-9042-7>.
- Haas, J., Zaworra, M., Glaubitz, J., Hertlein, G., Kohler, M., Lagojda, A., Lueke, B., Maus, C., Almanza, M.-T., Davies, T.G.E., Bass, C., Nauen, R., 2021. A toxicogenomics approach reveals characteristics supporting the honey bee (*Apis mellifera* L.) safety profile of the butenolide insecticide flupyradifurone. *Ecotoxicol. Environ. Saf.* 217, 112247. <https://doi.org/10.1016/j.ecoenv.2021.112247>.
- Haas, J., Glaubitz, J., Koenig, U., Nauen, R., 2022. A mechanism-based approach unveils metabolic routes potentially mediating chlorantraniliprole synergism in honey bees, *Apis mellifera* L., by azole fungicides. *Pest Manag. Sci.* 78 (3) <https://doi.org/10.1002/ps.6706>. Art. 3.
- Hamada, A., Wahl, G.D., Nesterov, A., Nakao, T., Kawashima, M., Banba, S., 2019. Differential metabolism of imidacloprid and dinotefuran by *Bemisia tabaci* CYP6CM1 variants. *Pestic. Biochem. Physiol.* 159, 27–33. <https://doi.org/10.1016/j.pestbp.2019.05.011>.
- Hemingway, J., 2018. Resistance: a problem without an easy solution. *Pestic. Biochem. Physiol.* 151, 73–75. <https://doi.org/10.1016/j.pestbp.2018.08.007>.
- Hemingway, J., Ranson, H., Magill, A., Kolaczinski, J., Fornadel, C., Ginnig, J., Coetzee, M., Simard, F., Roch, D.K., Hinzoumbe, C.K., Pickett, J., Schellenberg, D., Gething, P., Hoppé, M., Hamon, N., 2016. Averting a malaria disaster: will insecticide resistance derail malaria control? *Lancet* 387 (10029). [https://doi.org/10.1016/S0140-6736\(15\)00417-1](https://doi.org/10.1016/S0140-6736(15)00417-1). Art. 10029.
- Hoppé, M., Hueter, O.F., Bywater, A., Wege, P., Maienfisch, P., 2016. Evaluation of commercial agrochemicals as new tools for malaria vector control. *Chimia* 70 (10), 721–729. <https://doi.org/10.2533/chimia.2016.721>.
- Horstmann, S., Sonneck, R., 2016. Contact bioassays with phenoxybenzyl and tetrafluorobenzyl pyrethroids against target-site and metabolic resistant mosquitoes. *PLoS One* 11 (3). <https://doi.org/10.1371/journal.pone.0149738>. Art. 3.
- Ibrahim, S.S., Riveron, J.M., Bibby, J., Irving, H., Yunta, C., Paine, M.J.I., Wondji, C.S., 2015. Allelic variation of cytochrome P450s drives resistance to bednet insecticides in a major malaria vector. *PLoS Genet.* 11 (10) <https://doi.org/10.1371/journal.pgen.1005618>. Art. 10.
- Ibrahim, S.S., Amvongo-Adjia, N., Wondji, M.J., Irving, H., Riveron, J.M., Wondji, C.S., 2018. Pyrethroid resistance in the major malaria vector *Anopheles funestus* is exacerbated by overexpression and overactivity of the P450 CYP6AA1 across Africa. *Genes* 9 (3). <https://doi.org/10.3390/genes9030140>. Art. 3.
- Irving, H., Wondji, C.S., 2017. Investigating knockdown resistance (kdr) mechanism against pyrethroids/DDT in the malaria vector *Anopheles funestus* across Africa. *BMC Genet.* 18 (1), 76. <https://doi.org/10.1186/s12863-017-0539-x>.
- Khambay, B.P.S., 2002. Pyrethroid insecticides. *Pestic. Outlook* 13 (2), 49–54. <https://doi.org/10.1039/B202996K>.
- Khambay, B.P.S., Jewess, P.J., 2004. Pyrethroids (Bd. 6, S. 1–29). Elsevier Pergamon, London. <https://repository.rothamsted.ac.uk/item/895vq/pyrethroids>.
- Khan, M.F., Murphy, C.D., 2021. Cunninghamella spp. produce mammalian-equivalent metabolites from fluorinated pyrethroid pesticides. *AMB Express* 11, 101. <https://doi.org/10.1186/s13568-021-01262-0>.
- Manjon, C., Troczka, B.J., Zaworra, M., Beadle, K., Randall, E., Hertlein, G., Singh, K.S., Zimmer, C.T., Homem, R.A., Lueke, B., Reid, R., Kor, L., Kohler, M., Benting, J., Williams, M.S., Davies, T.G.E., Field, L.M., Bass, C., Nauen, R., 2018. Unravelling the molecular determinants of bee sensitivity to neonicotinoid insecticides. *Curr. Biol.* 28 (7) <https://doi.org/10.1016/j.cub.2018.02.045>. Art. 7.
- Mclaughlin, L.A., Niazi, U., Bibby, J., David, J.-P., Vontas, J., Hemingway, J., Ranson, H., Sutcliffe, M.J., Paine, M.J.I., 2008. Characterization of inhibitors and substrates of *Anopheles gambiae* CYP6Z2. *Insect Mol. Biol.* 17 (2) <https://doi.org/10.1111/j.1365-2583.2007.00788.x>. Art. 2.
- Nauen, R., Bass, C., Feyereisen, R., Vontas, J., 2022. The role of cytochrome P450s in insect toxicology and resistance. *Annu. Rev. Entomol.* 67 (1) <https://doi.org/10.1146/annurev-ento-070621-061328>. Art. 1.
- Nolden, M., Brockmann, A., Ebbinghaus-Kintscher, U., Brueggen, K.-U., Horstmann, S., Paine, M.J.I., Nauen, R., 2021. Towards understanding transfluthrin efficacy in a pyrethroid-resistant strain of the malaria vector *Anopheles funestus* with special reference to cytochrome P450-mediated detoxification. *Curr. Res. Parasitol. Vector-Borne Dis.* 1, 100041. <https://doi.org/10.1016/j.crvbd.2021.100041>.
- Nolden, M., Paine, M.J.I., Nauen, R., 2022a. Biochemical profiling of functionally expressed CYP6P9 variants of the malaria vector *Anopheles funestus* with special reference to cytochrome b5 and its role in pyrethroid and coumarin substrate metabolism. *Pestic. Biochem. Physiol.* 182, 105051. <https://doi.org/10.1016/j.pestbp.2022.105051>.
- Nolden, M., Paine, M.J.I., Nauen, R., 2022b. Sequential phase I metabolism of pyrethroids by duplicated CYP6P9 variants results in the loss of the terminal benzene moiety and determines resistance in the malaria mosquito *Anopheles funestus*. *Insect Biochem. Mol. Biol.* 148, 103813. <https://doi.org/10.1016/j.ibmb.2022.103813>.
- Ranson, H., Lissenden, N., 2016. Insecticide resistance in African *Anopheles* mosquitoes: a worsening situation that needs urgent action to maintain malaria control. *Trends Parasitol.* 32 (3), 187–196. <https://doi.org/10.1016/j.pt.2015.11.010>.

- Rinkevich, F.D., Du, Y., Dong, K., 2013. Diversity and convergence of Sodium Channel mutations involved in resistance to Pyrethroids. *Pestic. Biochem. Physiol.* 106 (3), 93–100. <https://doi.org/10.1016/j.pestbp.2013.02.007>.
- Riveron, J.M., Irving, H., Ndula, M., Barnes, K.G., Ibrahim, S.S., Paine, M.J.I., Wondji, C.S., 2013. Directionally selected cytochrome P450 alleles are driving the spread of pyrethroid resistance in the major malaria vector *Anopheles funestus*. *Proc. Natl. Acad. Sci.* 110 (1) <https://doi.org/10.1073/pnas.1216705110>. Art. 1.
- Riveron, J.M., Ibrahim, S.S., Chanda, E., Mzilahowa, T., Cuamba, N., Irving, H., Barnes, K.G., Ndula, M., Wondji, C.S., 2014. The highly polymorphic CYP6M7 cytochrome P450 gene partners with the directionally selected CYP6P9a and CYP6P9b genes to expand the pyrethroid resistance front in the malaria vector *Anopheles funestus* in Africa. *BMC Genomics* 15 (1). <https://doi.org/10.1186/1471-2164-15-817>. Art. 1.
- Riveron, J.M., Ibrahim, S.S., Mulamba, C., Djuouka, R., Irving, H., Wondji, M.J., Ishak, I.H., Wondji, C.S., 2017. Genome-wide transcription and functional analyses reveal heterogeneous molecular mechanisms driving Pyrethroids resistance in the major malaria vector *Anopheles funestus* across Africa. *G3 (Bethesda, Md.)* 7 (6). <https://doi.org/10.1534/g3.117.040147>. Art. 6.
- Scollon, E.J., Starr, J.M., Godin, S.J., DeVito, M.J., Hughes, M.F., 2009. In vitro metabolism of pyrethroid pesticides by rat and human hepatic microsomes and cytochrome P450 isoforms. *Drug Metab. Dispos.* 37 (1) <https://doi.org/10.1124/dmd.108.022343>. Art. 1.
- Scott, J.G., 2019. Life and death at the voltage-sensitive sodium channel: evolution in response to insecticide use. *Annu. Rev. Entomol.* 64 (1), 243–257. <https://doi.org/10.1146/annurev-ento-011118-112420>.
- Shono, T., Ohsawa, K., Casida, J.E., 1979. Metabolism of trans- and cis-permethrin, trans- and cis-cypermethrin, and decamethrin by microsomal enzymes. *J. Agric. Food Chem.* 27 (2) <https://doi.org/10.1021/jf60222a059>. Art. 2.
- Sinka, M.E., Bangs, M.J., Manguin, S., Coetzee, M., Mbogo, C.M., Hemingway, J., Patil, A.P., Temperley, W.H., Gething, P.W., Kabaria, C.W., Okara, R.M., Van Boeckel, T., Godfray, H.C.J., Harbach, R.E., Hay, S.I., 2010. The dominant *Anopheles* vectors of human malaria in Africa, Europe and the Middle East: occurrence data, distribution maps and bionomic précis. *Parasit. Vectors* 3 (1), 117. <https://doi.org/10.1186/1756-3305-3-117>.
- Sinka, M.E., Golding, N., Massey, N.C., Wiebe, A., Huang, Z., Hay, S.I., Moyes, C.L., 2016. Modelling the relative abundance of the primary African vectors of malaria before and after the implementation of indoor, insecticide-based vector control. *Malar. J.* 15 (1), 142. <https://doi.org/10.1186/s12936-016-1187-8>.
- Soderlund, D.M., 2020. Neurotoxicology of pyrethroid insecticides. In: *Advances in Neurotoxicology* (Bd. 4, S. 113–165). Elsevier. <https://doi.org/10.1016/bs.ant.2019.11.002>.
- Soderlund, D.M., Bloomquist, J.R., 1989. Neurotoxic actions of pyrethroid insecticides. *Annu. Rev. Entomol.* 34, 77–96. <https://doi.org/10.1146/annurev.en.34.010189.000453>.
- Stevenson, B.J., Bibby, J., Pignatelli, P., Muangnoicharoen, S., O'Neill, P.M., Lian, L.-Y., Müller, P., Nikou, D., Steven, A., Hemingway, J., Sutcliffe, M.J., Paine, M.J.I., 2011. Cytochrome P450 6M2 from the malaria vector *Anopheles gambiae* metabolizes pyrethroids: sequential metabolism of deltamethrin revealed. *Insect Biochem. Mol. Biol.* 41 (7) <https://doi.org/10.1016/j.ibmb.2011.02.003>. Art. 7.
- Suckling, C.J., 1988. The cyclopropyl group in studies of enzyme mechanism and inhibition. *Angew. Chem. Int. Ed. Eng.* 27 (4), 537–552. <https://doi.org/10.1002/anie.198805371>.
- Vontas, J., Katsavou, E., Mavridis, K., 2020. Cytochrome P450-based metabolic insecticide resistance in *Anopheles* and *Aedes* mosquito vectors: muddying the waters. *Pestic. Biochem. Physiol.* 170, 104666 <https://doi.org/10.1016/j.pestbp.2020.104666>.
- Wamba, A.N.R., Ibrahim, S.S., Kusimo, M.O., Muhammad, A., Mugenzi, L.M.J., Irving, H., Wondji, M.J., Hearn, J., Bigoga, J.D., Wondji, C.S., 2021. The cytochrome P450 CYP325A is a major driver of pyrethroid resistance in the major malaria vector *Anopheles funestus* in Central Africa. *Insect Biochem. Mol. Biol.* 138, 103647 <https://doi.org/10.1016/j.ibmb.2021.103647>.
- WHO, 2021. World Malaria Report, p. 2021. <https://www.who.int/teams/global-malaria-programme/reports/world-malaria-report-2021>.
- Williams, J., Flood, L., Praulins, G., Ingham, V.A., Morgan, J., Lees, R.S., Ranson, H., 2019. Characterisation of *Anopheles* strains used for laboratory screening of new vector control products. *Parasit. Vectors* 12 (1), Art. 1. <https://doi.org/10.1186/s13071-019-3774-3>.
- Wondji, C.S., Irving, H., Morgan, J., Lobo, N.F., Collins, F.H., Hunt, R.H., Coetzee, M., Hemingway, J., Ranson, H., 2009. Two duplicated P450 genes are associated with pyrethroid resistance in *Anopheles funestus*, a major malaria vector. *Genome Res.* 19 (3) <https://doi.org/10.1101/gr.087916.108>. Art. 3.
- Wondji, C.S., Hearn, J., Irving, H., Wondji, M.J., Weedall, G., 2022. RNAseq-based gene expression profiling of the *Anopheles funestus* pyrethroid-resistant strain FUM0Z highlights the predominant role of the duplicated CYP6P9a/b cytochrome P450s. *G3 Genes Genomes Genet.* 12 (1) <https://doi.org/10.1093/g3journal/jkab352>. Art. 1.
- Yoshida, T., 2012. Identification of urinary metabolites in rats administered the fluorine-containing pyrethroids metofluthrin, profluthrin, and transfluthrin. *Toxicol. Environ. Chem.* 94 (9), 1789–1804. <https://doi.org/10.1080/0272248.2012.729838>.
- Yoshida, T., 2014. Biomarkers for monitoring transfluthrin exposure: urinary excretion kinetics of transfluthrin metabolites in rats. *Environ. Toxicol. Pharmacol.* 37 (1), 103–109. <https://doi.org/10.1016/j.etap.2013.11.011>.